RESEARCH PAPER
Contrib. Sci. & Tech Eng, 2025, 2(3)
Homepage: https://cste.journals.umz.ac.ir/
DOI: 10.22080/cste.2025.28804.1019

Experimental Analysis, Statistical Modeling, and Optimization of the Edge Effects Associated with Laser-Bent Perforated Sheets

Mehdi Safari [1]

[1] *Associate Professor, Department of Mechanical Engineering, Arak University of Technology*

Article Info
Received 09 March 2025
Accepted 30 May 2025
Available online 20 July 2025

Keywords:
Laser bending process;
Perforated sheets;
Edge effect;
Statistical Analysis;
Optimization.

Abstract:
The edge effect phenomenon is instrumental in influencing the precision, reliability, and overall caliber of laser-bent sheets. This study conducts an experimental investigation into the edge effect present in laser-bent perforated sheets. To this end, the impact of critical input parameters in the laser bending process, including laser output power, laser scanning speed, and the number of irradiations on the edge effect of laser-bent perforated sheets, is meticulously assessed. The findings indicate that the edge effect phenomenon intensifies with an increase in laser power. Furthermore, it is observed that the edge effect diminishes as the laser scanning speed escalates. Additionally, an increase in the number of irradiations correspondingly enhances the edge effect of perforated sheets. The optimization of input parameters reveals that to attain the minimal edge effect in laser bent perforated sheets, the laser output power, scanning speed, and number of irradiations must be calibrated to 90 Watts, 3 mm/s, and 10, respectively an edge effect of merely 1.25% at the free edge of the LBPS can be successfully achieved.

© 2025 University of Mazandaran

***Corresponding Author:** m.safari@arakut.ac.ir

Supplementary information: Supplementary information for this article is available at https://cste.journals.umz.ac.ir/

Please cite this paper as: Safari, M. (2025). Experimental analysis, statistical modeling and optimization of the edge effects associated with laser-bent perforated sheets. Contributions of Science and Technology for Engineering, 2(3), 37-44. doi:10.22080/cste.2025.28804.1019

1. Introduction

In recent years, the application of laser beam technology for bending sheets and tubes has seen significant growth across various industries. This method has gained widespread recognition due to its exceptional precision, elimination of spring-back, and minimal impact on the material's microstructure. Unlike conventional mechanical bending techniques, laser bending absorbs thermal energy to induce deformation. The energy from the laser beam generates localized thermal expansion, leading to plastic deformation during the cooling phase. Numerous studies have explored different aspects of the laser bending process (LBP).

Liu et al. [1] conducted an investigation into the LBP in stainless steel foils to fabricate negative bending angles empirically. Their findings indicated that augmenting the pre-stresses applied to the sheet significantly enhances the magnitude of the negative bending angle. Shen et al. [2], through the execution of FEM simulations and empirical experiments, endeavored to advance the comprehension of the edge effect phenomenon associated with the LBP. To mitigate the edge effect in LBP, they proposed scanning methodologies wherein the velocity was modulated along the irradiation trajectory. Kant and Joshi [3] investigated the LBP of magnesium alloy to attain bending angles exceeding 10 degrees. Their outcomes revealed that the frequency of laser irradiation scans significantly impacts the deformation characteristics of the laser-bent magnesium sheet. Wang et al. [4] analyzed the underlying mechanism of the bending process in the LBP of a metal composite plate utilizing the FEM simulations. To regulate the bending behavior as well as the edge effect in LBP, they proposed four distinct scanning strategies that enhanced the precision of the forming process. Nath et al. [5] utilized a coupled thermal-mechanical FEM simulation to examine the bending behavior of magnesium alloy sheets subjected to laser irradiation. The principal finding from their research indicated that the bending angle observed in a multi-pass scheme was 430% greater than that recorded in a single-pass irradiation scheme. Zhang et al. [6] introduced a variable velocity scheme to alleviate the edge effect in the LBP of DP-980 steel. They concluded that employing the variable velocity scheme significantly the reduced free edge of the laser-bent sheet. Song et al. [7] investigated the bending of high-strength steels through experimental trials and finite element simulations, discovering that an increased absorption coefficient significantly enhances the bending angle. Maji et al. [8] conducted experimental research on stainless steel sheets, analyzing the influence of process variables, particularly the number of irradiation passes, through mechanical and metallurgical assessments. Their study determined an optimal condition for maximizing the bending angle, revealing that laser bending refines the

© 2025 by the authors. Licensee CSTE, Babolsar, Mazandaran. This article is an open access article distributed under the terms and conditions of the Creative Commons Attribution (CC-BY) license (https://creativecommons.org/licenses/by/4.0/deed.en)

*ISSN **3060-6578***

microstructure and increases micro-hardness in the deformed area. Fetene et al. [9] compared the bending angles of cement-coated and friction stir-processed sheets under laser irradiation, concluding that both exhibited increased absorption coefficients. In a separate study, Fetene et al. [10] examined how sheet dimensions impact bending behavior in AH36 steel, finding that increasing sheet width and reducing thickness resulted in higher bending angles. Paramasivan et al. [11] explored the role of forced cooling in LBP using numerical simulations, establishing that external cooling enhances the bending angle. Safari and Joudaki [12] applied artificial neural networks to predict bending angles in tailored machined blanks (TWB), demonstrating that neural networks offer highly accurate predictions. Additional studies have examined specialized applications of LBP. Kotobi et al. [13] analyzed residual stress distribution in steel-titanium laminated sheets, showing that tensile stresses increase with higher laser power. Seyedkashi et al. [14] examined LBP in SUS304L/C11000 clad sheets, assessing the influence of scanning speed, laser power, and beam diameter on bending performance. Li et al. [15] derived an analytical model to predict bending angles in laminated sheets by calculating temperature gradients, demonstrating close agreement with experimental findings. Yadav et al. [16] investigated the ramifications of instituting forced cooling on the surface that is opposed to the one undergoing laser irradiation during the LBP. In pursuit of this objective, they developed a FEM model to evaluate the effects of forced cooling. Their results indicated that implementing forced cooling could significantly augment the bending angle. Mazdak et al. [17] concentrated on the LBP of bilayer aluminum-steel sheets, utilizing statistical models to analyze how varying laser parameters influenced the resultant bending angles. Their investigation integrated both experimental and computational methodologies. The variance analysis revealed that the laser power exerted the most pronounced influence on the bending angle. Rattan et al. [18] executed a numerical analysis to explore the implications of applying a coating on the surface subjected to laser irradiation during the LBP. They employed a lime coating on the irradiated surface, and their outcomes illustrated that this coating increased bending of the sheet while concurrently reducing residual stresses. Abedi et al. [19] contrasted the effects of surface roughness and the application of a coating on the irradiated surface regarding laser beam absorption and bending angle. They applied a Cr2O3 oxide layer to the irradiated surface. Their results indicated that both augmented surface roughness and increased coating thickness had a significant influence on the bending angle.

The phenomenon known as the laser-induced edge effect that occurs during the laser bending process is of paramount importance, as it plays a critical role in determining the accuracy, consistency, and overall quality of the final manufactured product, which is essential for meeting industry standards and customer expectations. This intricate effect emerges from the complex interactions that take place between the laser beam and the edges of the metal sheet, resulting in a variety of unique and significant changes in the thermal, mechanical, and microstructural characteristics of the material being processed.

A review of the literature highlights the effectiveness of LBP for precision bending applications. While extensive research has been conducted on various materials, limited studies have addressed the laser bending of perforated sheets. On the other hand, considering the significance of the edge effect in laser-bent sheets, based on the author's knowledge, no reports have been presented regarding the edge effect in laser-bent perforated sheets. Therefore, this article investigates the edge effect in laser-bent perforated sheets. Traditional die-based bending methods often result in hole distortion and ovalization along the bend line, presenting challenges in maintaining dimensional accuracy. By leveraging LBP, this study examines how process parameters—such as laser output power (LOP), laser scanning speed (LSS), and number of irradiations (NIS) affect the edge effects of perforated sheets.

2. Experimental work

For conducting the experimental tests, a continuous-wave CO_2 laser system maximum output power of 120 Watts is employed. The experiments are performed on mild steel sheets with dimensions of 75×50×1 mm. The chemical composition of mild steel is presented in Table 1.

Table 1. The chemical composition of mild steel

Element	Fe	C	Cu	Mn	P	Si
Content (%)	98.0	0.26	0.20	0.93	0.04	0.28

To enhance laser energy absorption, the surface of the samples is coated with graphite powder. The experimental setup for the LBP and a laser-bent perforated sheet is illustrated in Figure 1.

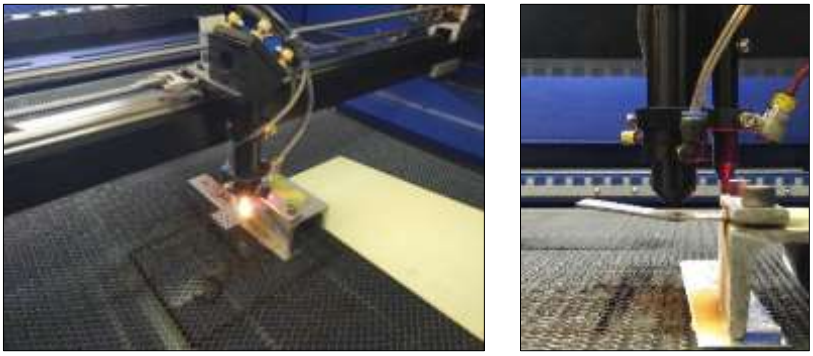

Figure 1. The experimental setup for the LBP and a laser-bent perforated sheet

Three critical process parameters identified as significantly influencing the edge effect of LBPS are the LOP, the LSS, and the NIS. To accurately determine the appropriate range of these input parameters specifically for the LBP applied to perforated sheets, a series of meticulously designed experiments is conducted. It is essential to recognize that three distinct levels are meticulously considered for each parameter. The specific levels associated with each input parameter pertinent to the current investigation are comprehensively presented in Table 2.

Table 2. The levels of each input parameter for the LBP of the perforated sheet

Input Variables	Symbol	Min Value	Mid Value	Max Value
LOP [Watts]	P	90	102	114
LSS [mm/s]	S	1	2	3
NIS	N	10	15	20

It is imperative to highlight that during the experimental procedure, after each step of irradiation, a sufficient duration is allocated to allow the perforated sheet to cool down to room temperature before proceeding with the subsequent steps. Furthermore, the positioning of the laser spot is strategically placed at a point situated above the surface that is being irradiated, which consequently results in the generation of a laser beam possessing a radius of 1 mm upon the surface of the sheet. The Response Surface Methodology (RSM) is employed as a sophisticated statistical tool to ascertain the effects of the process parameters and the interactions that exist among them on the resulting output. Nevertheless, in the context of the present study, the RSM utilizing the Box-Behnken design is specifically implemented to systematically arrange the experiments, culminating in 15 distinct experimental trials being executed. The detailed outline of the experiments that are planned to be conducted is illustrated in Table 3.

Table 3. The experiments based on the Box-Behnken design

Experiment number	P	S	N
1	90	1	15
2	114	1	15
3	90	3	15
4	114	3	15
5	90	2	10
6	114	2	10
7	90	2	20
8	114	2	20
9	102	1	10
10	102	3	10
11	102	1	20
12	102	3	20
13	102	2	15
14	102	2	15
15	102	2	15

To guarantee the reproducibility and reliability of the experimental results, all tests delineated in Table 3 are conducted three times. A coordinate measuring machine is employed to facilitate the measurement of the vertical displacements (Y-displacements) of the sheet. For this measurement, the Y-displacements at five strategically selected points along the free edge are meticulously recorded. The edge effect, which reflects variations in the bending angle along the free edge, is quantified by the difference between the maximum and minimum vertical displacements, as defined in Equation 1.

$$\text{Edge Effect } (\%) = \frac{Y_{max} - Y_{min}}{Y_{max}} \times 100 \quad (1)$$

3. Results and discussion

After conducting a meticulous measurement of the Y-displacements associated with the LBPS and calculating the edge effects, the subsequent results derived from the comprehensive analysis of variance, commonly referred to as ANOVA, were carefully analyzed and systematically presented in Table 4. It should be noted that, within the confines of Table 4, the parameters that yield a P-value of less than 0.05 are deemed to be significant effective parameters influencing the edge effect of the LBPS. Furthermore, it is essential to highlight that elevated F-values indicate a more pronounced influence exerted by the input parameters on the edge effect of the sheet that has undergone the bending process.

Table 4. The results of the analysis of variance (ANOVA) for the edge effect of LBPS

Source	DF	Seq SS	Contribution (%)	Adj SS	Adj MS	F-Value	P-Value
Model	5	3.19762	99.69	3.19762	0.63952	571.40	0.000
Linear	3	3.17125	98.86	1.82110	0.60703	542.37	0.000
LOP	1	1.53125	47.74	0.18110	0.18110	161.80	0.000
LSS	1	1.21680	37.93	1.21680	1.21680	1087.18	0.000
NIS	1	0.42320	13.19	0.42320	0.42320	378.12	0.000
Square	2	0.02637	0.82	0.02637	0.01319	11.78	0.003
LOP*LOP	1	0.02120	0.66	0.01963	0.01963	17.54	0.002
LSS*LSS	1	0.00517	0.16	0.00517	0.00517	4.62	0.060
Error	9	0.01007	0.31	0.01007	0.00112		
Lack-of-Fit	7	0.00821	0.26	0.00821	0.00117	1.26	0.512

Pure Error	2	0.00187	0.06	0.00187	0.00093
Total	14	3.20769	100		

A Pareto chart was meticulously plotted based on the results, as illustrated in Figure 2.

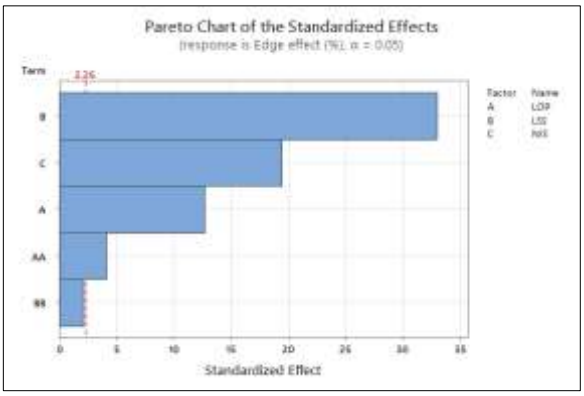

Figure 2. The Pareto chart for the edge effect of LBPS

From the detailed examination of Table 4, it is evident that the LOP emerges as the most critical parameter impacting the edge effect of the perforated sheet, followed in importance by the LSS. Ultimately, the NIS is identified as the third parameter of significance affecting the edge effect. The edge effect of the LBPS can be mathematically expressed by the equation denoted as Equation 2, which is appropriate and valid for the specific range of input parameters delineated in Table 2.

$$\text{Edge effect (\%)} = -6.42 + 0.1394\ \text{LOP} - 0.5392\ \text{LSS} + 0.04600\ \text{NIS} - 0.000505\ \text{LOP*LOP} + 0.0373\ \text{LSS*LSS} \quad (2)$$

The coefficient of determination, commonly referred to as "R^2," is a quantitative measure used to assess the percentage of concordance between the data predicted by the statistical model and the actual experimental data. In the context of a theoretically perfect statistical model, the ideal value of R^2 is established as 1. In this instance, the coefficient of determination (R^2) was calculated to be 0.9982 for the response reflecting the edge effect of the free edge of the LBPS, which compellingly indicates that the predictive model is capable of forecasting 99.82% of the experimental data while relegating a mere 0.18% of the total variations as being unexplained. In Figure 3, the residual plots pertinent to the implemented model are meticulously showcased.

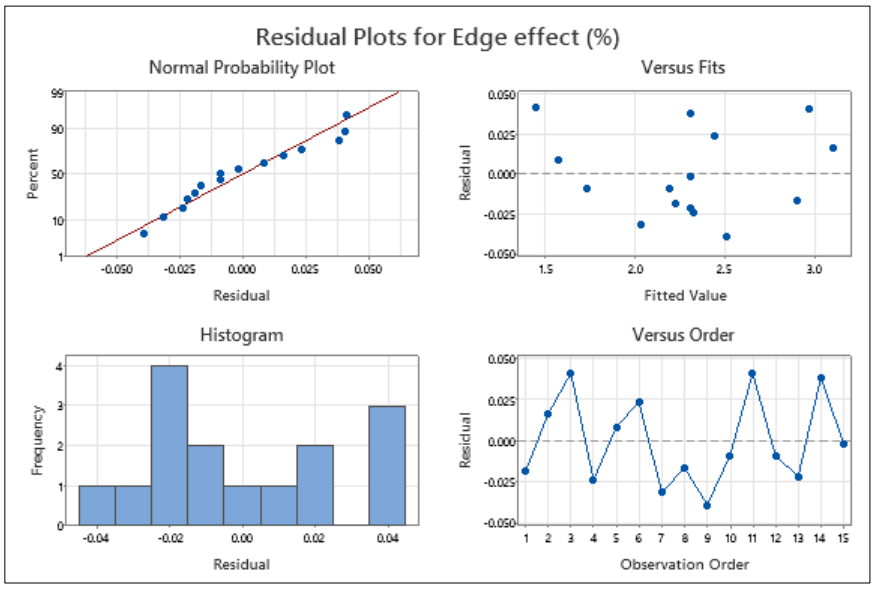

Figure 3. The residual plots pertinent to the implemented model are meticulously showcased

As evidenced in Figure 3, the normal probability plot indicates that the residuals exhibit a normal distribution and closely approximate a straight line. Moreover, it has been substantiated through the residuals versus fits graph that the residuals are distributed randomly, devoid of any discernible patterns within the data. The analysis of the histogram leads to the conclusion that the data do not exhibit skewness. The results derived from the residuals versus order graph further indicate the absence of trends or patterns, thereby substantiating the independence of the residuals from one another. It has been convincingly demonstrated through the analysis presented in Figure 3 that the edge effect of the LBPS can be accurately predicted by the model employed in this study. Nevertheless, as illustrated in Figure 4, the ramifications of varying input parameters on the edge effect of the free edge of an LBPS are meticulously delineated and portrayed comprehensively.

The influence exerted by the LOP on the edge effect phenomenon is vividly represented in Figure 4. From a thorough examination of the data presented in this figure, one can conclude that an increase in the LOP correlates positively with a rise in the edge effects observed. This relationship can be attributed to the fact that the rate of heat transfer is intrinsically linked to both the input heat flux and the temperature profile of the sheet material. Consequently,

with a heightened rate of heat transfer occurring at elevated levels of laser power, a greater expanse of the sheet surface becomes exposed to thermal energy. It is worth noting that initially, the sheet commences at ambient temperature at the onset of the irradiation path, whereas the temperature progressively increases towards the conclusion of this irradiation path due to ongoing heat transfer processes. This results in distinct regions within the sheet that exhibit disparate boundary conditions and thermal states. Thus, the edge effect is amplified in conjunction with an increase in the LOP. Upon careful observation of the data depicted in Figure 4, it becomes evident that there is an inverse relationship between the edge effect and the LSS, specifically indicating that as the LSS increases, a corresponding decrease in the edge effect is observed. The rationale behind this phenomenon lies in the quantity of thermal energy transferred to the sheet is diminished as the scanning speed is increased, which consequently leads to a reduction in the areas of the sheet that are subjected to laser-induced heating. This reduction in thermal exposure results in fewer regions experiencing the effects of varying boundary conditions and thermal states. Therefore, it can be conclusively stated that the edge effects experienced by the sheet are significantly attenuated as the LSS is elevated. From a thorough examination of the data presented in Figure 4, one can conclude that an increase in the NIS correlates positively with a rise in the edge effects observed. Each pulse emitted by the laser beam serves to introduce a significant increment of thermal energy into the material being processed, thereby affecting its physical properties. While our primary aim remains the attainment of a predetermined curvature within the material, it is important to note that the heat generated by the laser pulse also propagates to surrounding areas, with a pronounced effect observed particularly in the regions located near the edges of the material. Moreover, it is essential to recognize that the edges of the material typically represent zones characterized by rapid temperature fluctuations, commonly referred to as high thermal gradients. As each successive laser pulse is applied, these thermal gradients become increasingly pronounced and intensify in their severity. The presence of such steep thermal gradients ultimately results in a differential expansion and contraction of the material, which, in turn, induces a significant degree of deformation and generates stress concentrations specifically at the edges of the material. In the subsequent analysis, the intricate contour plots that illustrate the various interactions between the input parameters are meticulously examined. Figures 5 to 7 present a comprehensive depiction of the interactions that occur between the variables LOP, LSS, and NIS alongside their consequential effects on the edge effects observed at the free edge of the laser-bent perforated sheet.

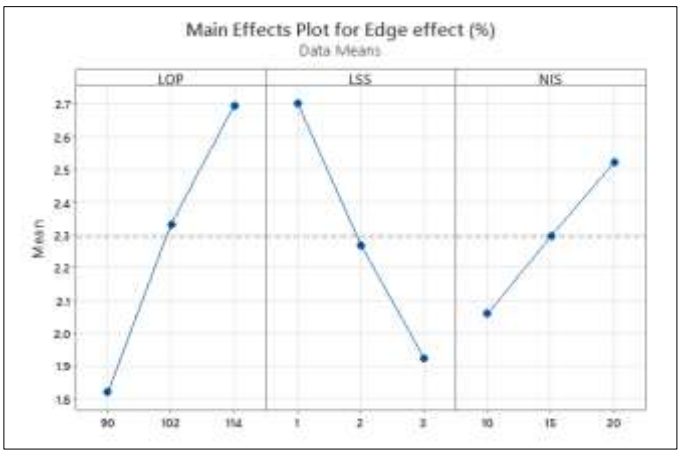

Figure 4. **Effects of input parameters on the edge effect of LBPS**

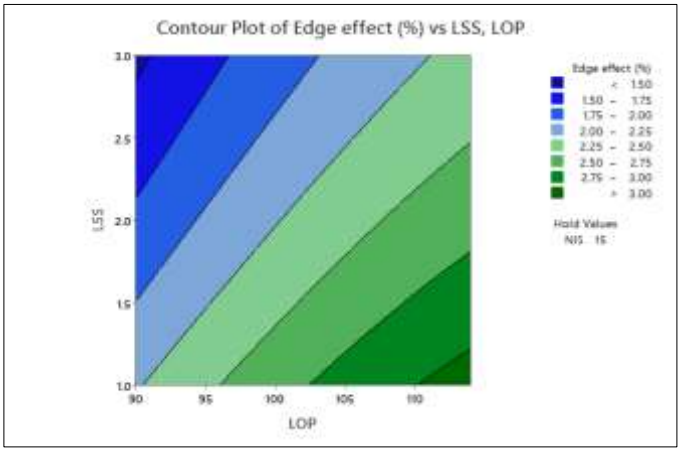

Figure 5. **Interaction plot of LOP and LSS for the edge effect of LBPS**

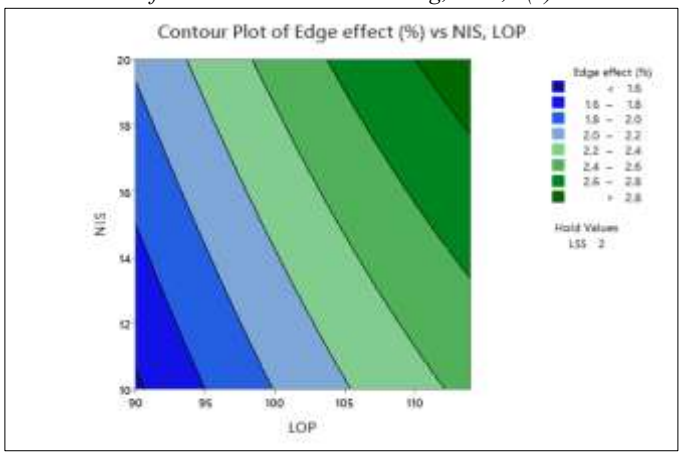

Figure 6. **Interaction plot of LOP and NIS for the edge effect of LBPS**

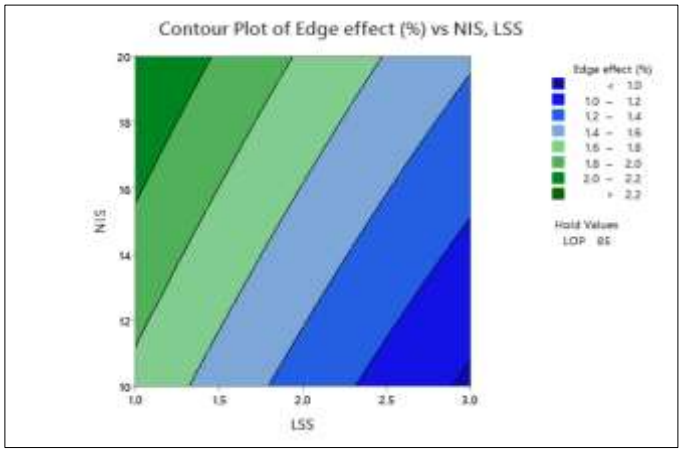

Figure 7. **Interaction plot of LSS and NIS for the edge effect of LBPS**

Upon close inspection, it becomes evident that the conditions under which the minimum edge effects can be achieved are characterized by the simultaneous occurrence of the minimum possible values for both LOP and NIS, while concurrently maintaining the LSS at its maximum possible value.

3.1. Optimization of Edge Effect in LBPS

Figure 8 illustrates the most favourable conditions for various process parameters, which encompass the LOP, the LSS, and the NIS, all of which are crucial for attaining the minimal edge effect observed at the free edge of the LBPS. The primary objective of this segment of the study is to meticulously evaluate the extent to which each input parameter must be judiciously selected within the specified ranges delineated in Table 2 to effectively minimize the edge effect that manifests in the perforated sheet that has been manipulated through the application of laser technology.

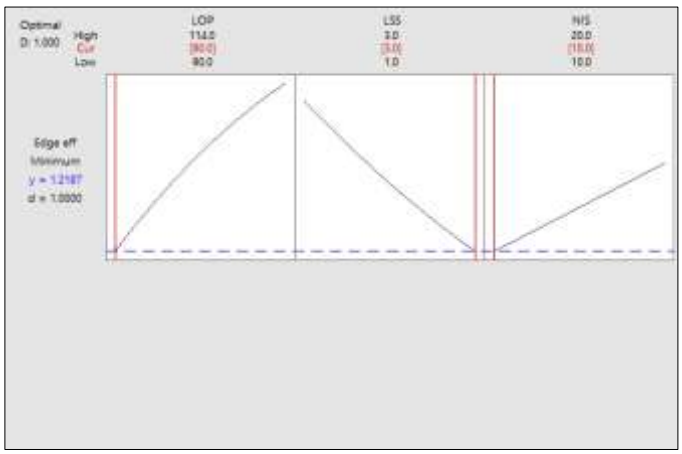

Figure 8. **The optimal conditions of LOP, LSS, and NIS for achieving the minimum edge effect**

Upon thorough examination of the identified optimal conditions, the resultant findings can be summarized as follows: by establishing the LOP at a value of 90 Watts, configuring the LSS to exactly 3 mm/s, and determining the NIS to be 10, one can achieve a notably reduced edge effect in the laser-bent sheet, which is quantified at an impressive rate of merely 1.22%.

4. Conclusion

In this article, the in-depth experimental investigation of the LBP of perforated sheets has been thoroughly examined and discussed in detail. To achieve this objective, a comprehensive analysis was conducted focusing on the influence of various process parameters, which include LOP, LSS, and NIS, on the resultant effects produced by the process, particularly regarding the edge effect observed in the LBPS. The methodologies employed for statistical modeling and optimization were integral to exploring how these process parameters affect the edge effect manifested in the bent sheets, thus enabling a more robust understanding of the underlying mechanisms at play. Furthermore, to facilitate a precise and holistic examination of the impact of these process parameters, including the intricate interaction effects between input parameters on the edge effect, the Design of Experiments (DOE) methodology grounded in RSM was meticulously employed. As a culmination of this extensive research endeavor, the following significant results were derived:

– The findings of this investigation indicated that an increase in the LOP is positively correlated with an enhancement in the edge effect associated with the LBPS, thereby suggesting a direct relationship between these two variables.

– Moreover, it was conclusively determined from the analytical results that an elevation in the LSS results in a marked reduction in the edge effect of the LBPS, indicating a counteractive relationship between these parameters.

– Additionally, it was rigorously demonstrated that an increase in the NIS correlates positively with an enhancement in the perforated sheet's edge effect, thereby underscoring this parameter's significance in the overall process dynamics.

– The optimization of the input parameters aimed at attaining the minimum edge effect in the LBPS revealed that by calibrating the LOP to a precise value of 90 Watts, setting the LSS to 3 mm/s, and establishing the NIS at 10 passes, an edge effect of merely 1.25% at the free edge of the LBPS can be successfully achieved.

5. References

[1] Liu, J., Sun, S., Guan, Y., & Ji, Z. (2010). Experimental study on negative laser bending process of steel foils. Optics and Lasers in Engineering, 48(1), 83–88. doi:10.1016/j.optlaseng.2009.07.019.

[2] Shen, H., Hu, J., & Yao, Z. (2010). Analysis and control of edge effects in laser bending. Optics and Lasers in Engineering, 48(3), 305–315. doi:10.1016/j.optlaseng.2009.11.005.

[3] Kant, R., & Joshi, S. N. (2016). Thermo-mechanical studies on bending mechanism, bend angle and edge effect during multi-scan laser bending of magnesium M1A alloy sheets. Journal of Manufacturing Processes, 23, 135–148. doi:10.1016/j.jmapro.2016.05.017.

[4] Wang, X., Shi, Y., Guo, Y., & Sun, R. (2020). Laser bending and edge effect control of layered metal composite plate. Chinese Journal of Lasers, 47(3), 302004-1. doi:10.3788/cjl202047.0302004

[5] Nath, U., Yadav, V., & Purohit, R. (2021). Finite element analysis of AM30 magnesium alloy sheet in the laser bending process. Advances in Materials and Processing Technologies, 8(2), 1803–1815. doi:10.1080/2374068x.2021.1878699.

[6] Zhang, Y., Dong, W., Yang, T., Guo, C., & Chen, F. (2022). Edge effect reduction in laser bending of DP980 high-strength steel. International Journal of Advanced Manufacturing Technology, 119(3–4), 1965–1973. doi:10.1007/s00170-021-08424-1.

[7] Song, J. H., Lee, G. A., Jung, K. H., & Park, S. J. (2015). Laser irradiated bending characteristics of the ultra-high strength steel sheets. International Journal of Automotive Technology, 16(1), 89–96. doi:10.1007/s12239-015-0010-9.

[8] Maji, K., Pratihar, D. K., & Nath, A. K. (2016). Experimental investigations, modeling, and optimization of multi-scan laser forming of AISI 304 stainless steel sheet. International Journal of Advanced Manufacturing Technology, 83(9–12), 1441–1455. doi:10.1007/s00170-015-7675-0.

[9] Fetene, B. N., Dixit, U. S., & Liao, H. (2017). Laser bending of friction stir processed and cement-coated sheets. Materials and Manufacturing Processes, 32(14), 1628–1634. doi:10.1080/10426914.2017.1279321.

[10] Fetene, B. N., Kumar, V., Dixit, U. S., & Echempati, R. (2018). Numerical and experimental study on multi-pass laser bending of AH36 steel strips. Optics & Laser Technology, 99, 291–300. doi:10.1016/j.optlastec.2017.09.014.

[11] Paramasivan, K., Das, S., Marimuthu, S., & Misra, D. (2018). Increment in laser bending angle by forced bottom cooling. International Journal of Advanced Manufacturing Technology, 94(5–8), 2137–2147. doi:10.1007/s00170-017-1035-1.

[12] Safari, M., & Joudaki, J. (2018). Prediction of Bending Angle for Laser Forming of Tailor Machined Blanks by Neural Network. Iranian Journal of Materials Forming, 5(1), 45–57. doi:10.22099/ijmf.2018.28561.1097.

[13] Kotobi, M., & Honarpisheh, M. (2018). Through-depth residual stress measurement of laser bent steel–titanium bimetal sheets. Journal of Strain Analysis for Engineering Design, 53(3), 130–140. doi:10.1177/0309324717753212.

[14] Seyedkashi, S. M. H., Abazari, H. D., Gollo, M. H., Woo, Y. Y., & Moon, Y. H. (2019). Characterization of laser bending

of SUS304L/C11000 clad sheets. Journal of Mechanical Science and Technology, 33(7), 3223–3230. doi:10.1007/s12206-019-0617-2.

[15] Li, Z., & Wang, X. (2019). Analytical model for estimating bending angle in laser bending of 304 stainless steel/Q235 carbon steel laminated plate. Journal of Laser Applications, 31(4), 42012. doi:10.2351/1.5116729.

[16] Yadav, R., Goyal, D. K., & Kant, R. (2022). Enhancing process competency by forced cooling in laser bending process. Journal of Thermal Stresses, 45(8), 617–629. doi:10.1080/01495739.2022.2103057.

[17] Mazdak, S., Sheykholeslami, M. R., Gholami, M., Parvaz, H., Najafizadeh, M. M., Mahmoudi, S., & Vanaki, A. (2023). A statistical model for estimation of bending angle in laser bending of two-layer steel-aluminum sheets. Optics & Laser Technology, 157, 108575. doi:10.1016/j.optlastec.2022.108575.

[18] Rattan, A., Jasra, Y., & Saxena, R. K. (2020). Prediction of bending behavior for laser forming of lime coated plain carbon steel using finite element method. Materials Today: Proceedings, 28, 1943–1950. doi:10.1016/j.matpr.2020.05.411.

[19] Abedi, H. R., & Hoseinpour Gollo, M. (2019). An experimental study of the effects of surface roughness and coating of Cr2O3 layer on the laser-forming process. Optics & Laser Technology, 109, 336–347. doi:10.1016/j.optlastec.2018.07.064.